Ocean Engineering 342 (2025) 123029

Contents lists available at ScienceDirect

Ocean Engineering

journal homepage: www.elsevier.com/locate/oceaneng

Research paper

Considerations on the superposition method's applicability to pile group impedance functions for offshore wind turbine foundations

Eduardo Rodríguez-Galván, Guillermo M. Álamo *, Juan J. Aznárez, Orlando Maeso

Instituto Universitario de Sistemas Inteligentes y Aplicaciones Numéricas en Ingeniería (SIANI), Universidad de Las Palmas de Gran Canaria, 35017, Las Palmas de Gran Canaria, Spain

ARTICLE INFO

Keywords:
Pile-soil-pile model
Pile groups
Impedance functions
Dynamic analysis
Elastic superposition method
Offshore wind turbines

ABSTRACT

The modelling of pile-soil-pile interaction using the superposition method is studied. For this purpose, a general matrix-based formulation is implemented, explicitly incorporating all flexibility components of the problem: horizontal, rocking, vertical, and their coupled terms. This model is employed to: (1) investigate the impact of each individual flexibility terms, by selectively removing them within the global formulation, on the horizontal, rocking, and cross-coupled impedances functions; and (2) evaluate the method's applicability to polygonal pile group configurations, representative of those used in jacket-supported offshore wind turbines. A previously developed continuum model has been used as a benchmark for validation. Results show that the horizontal, cross-coupled and rocking dynamic impedances for regular pile groups are accurately reproduced through the superposition method. It is revealed that the horizontal impedances are correctly estimated when the terms related to vertical behaviour are neglected, by only considering the horizontal and rocking flexibilities. The rocking impedances are mainly influenced by the vertical component, although the flexibility terms related to the vertical-lateral coupling can be disregarded. However, to correctly reproduce the group cross-coupled impedances, all vertical, horizontal, rocking, and their coupling flexibility terms must be considered.

1. Introduction

Offshore wind energy has emerged as a key source of renewable power in the pursuit of a sustainable future. In recent years, the installation of Offshore Wind Turbines (OWTs) has been increasing. According to the 2024 Global Offshore Wind Report (GWEC, 2024), 2023 was the second highest year in terms of OWT installations, incorporating 11 GW of offshore wind power into the grid, reaching at the end of this year a total offshore wind capacity of 75 GW. Even with the current challenges that are affecting the world market and economy, such as supply chain issues, rising inflation, and high interest rates, offshore wind installations are expected to continue growing in the coming years. Attending to the predictions of this report (GWEC, 2024), nearly 380 GW of offshore wind capacity will be added during the next decade. These OWTs can be supported by several structure typologies, which can be substructures directly founded on the seabed or floating platforms. Despite floating OWTs had been acquiring interest in recent years, they are currently in development, presenting higher costs than the directly founded solutions. For this reason, it is also predicted that in the coming years the majority of the new installed power will be mainly represented by directly founded substructures. Among these substructure typologies, monopiles are the predominant foundation, due to their ease of installation and lower production costs. Attending to the Offshore Wind Market Report (McCoy et al., 2024), 55.6 % of the installed OWTs are supported by monopiles. Afterwards, jacket substructures are the second most common substructure typology, with a representation of 13.4 % of the installed OWTs, followed by pile caps (7.6 %) and tripods (1.6 %). Jacket representation is expected to increase in the coming years due to the need to install OWTs further from the coast. These substructures are structurally more efficient than monopiles for installing OWTs in deeper seabed depths. Jackets are founded on group of several (generally between 3 and 5) piles or suction caissons forming a polygonal configuration. While suction caissons have become more popular due to their quieter installation process and ease of deployment, pile groups offer greater versatility in terms of soil conditions and higher bearing capacity thanks to their larger slenderness. Due to all these factors, pile groups, which are also extensively employed in a broad range of structure foundations, have gained significant popularity as OWT foundations.

As a consequence of the great versatility of pile groups serving as foundations, the response of pile groups under dynamic loads has been widely analysed throughout the years, being an essential factor to

* Corresponding author.
E-mail addresses: eduardo.rodriguezgalvan@ulpgc.es (E. Rodríguez-Galván), guillermo.alamo@ulpgc.es (G.M. Álamo), juanjose.aznarez@ulpgc.es (J.J. Aznárez), orlando.maeso@ulpgc.es (O. Maeso).

https://doi.org/10.1016/j.oceaneng.2025.123029
Received 2 August 2025; Received in revised form 9 September 2025; Accepted 28 September 2025
Available online 8 October 2025

ensure the efficient design and safe of the whole structural system (Abhinav and Saha, 2015; Jalbi and Bhattacharya, 2018; Plodpradit et al., 2019; Romero-Sánchez and Padrón, 2024; Quevedo-Reina et al., 2024). The dynamic response of pile groups refers to the coupled behaviour of the entire group and the surrounding soil. In this way, two complex phenomena are presented within this problem: pile-soil and pile-soil-pile interaction. This dynamic response can be addressed by assuming a non-linear or linear soil-structure interaction modelling. On the one hand, non-linear models reproduce pile-soil interaction by means of soil resistance-deflection curves ($p-y$, $t-z$, $q-z$ curves), which are capable to capture plastic behaviour under cyclic loads, stiffness degradation, hysteresis, or other effects such as soil gapping. In these modes, pile-soil interaction is usually reproduced by Beam on Dynamic Winkler Foundation models, where the pile is modelled as a beam and the surrounding soil through distributed non-linear springs and dashpots. For pile groups, pile-soil-pile interaction is usually quantified by employing p-multipliers, which reduce the $p-y$ relationship of a single pile to account for shadowing effects, group efficiency, and other non-linear aspects within the group. Because this non-linear modelling realistically simulates soil-structure interaction, it has been and continues to be widely applied in OWT dynamic analyses (Kim et al., 2014; Bisoi and Haldar, 2015; Yang et al., 2019; Ali et al., 2021; Shi et al., 2022). However, it requires high-computational effort, and an extensive geotechnical characterization. This may represent a limitation when addressing the initial phases of structural design or when conducting parametric studies that involve the assessment of numerous scenarios. On the other hand, linear models assume constant stiffness and damping independent of deflection. In the dynamic analysis of OWT, linear models usually reproduce pile-soil interaction by frequency-dependent impedance functions, whereas pile-soil-pile interaction is treated using superposition techniques or empirical interaction factors. They are simplified models, and their main advantage is their computational efficiency, enabling them to perform large number of simulations, which is particularly valuable for preliminary design and parametric studies. It is primarily in this context that they have been employed within the dynamic analysis of OWT structures (Medina et al., 2021; Padrón et al., 2022; Romero-Sánchez and Padrón, 2024; Kaynia et al., 2025). Once feasible foundation configurations are identified, non-linear models can then be employed in detailed design stages to refine predictions under extreme or critical load conditions.

For both assumptions (non-linear and linear) the coupled behaviour between pile-soil and pile-soil-pile interaction can be reproduced by advanced rigorous models. Nevertheless, for the linear modelling the superposition of elastic effects can also be used. On the one hand, advanced models (Kaynia, 1982; Kaynia and Kausel, 1991; Dezi et al., 2009, 2016; Álamo et al., 2016; Wang et al., 2017) employ sophisticated numerical techniques to reproduce pile-soil-pile and pile-soil interaction phenomena. The finite and boundary element methods are usually used to account for these effects. Advanced models can be based on linear or non-linear assumptions, providing an accurate analysis but requiring a high computational effort. On the other hand, the elastic superposition method (Poulos, 1968; Dobry and Gazetas, 1988; Gazetas and Makris, 1991; Mylonakis and Gazetas, 1998a; Makris and Gazetas, 1992; Rotta Loria and Laloui, 2016; Dai et al., 2017; Luan et al., 2020; Rodríguez-Galván et al., 2025) is a simplified approach that allows computing the static and dynamic response of pile groups in a straightforward way. In this method the overall group behaviour is obtained by superimposing single pile and pile pair responses, neglecting the influence that the other piles in the group may have on these responses. This simplified method assumes a linear elastic behaviour of the media involved in the problem.

The elastic superposition method was firstly presented by Poulos (1968). This work introduced the interaction factor concept in order to quantity pile-soil-pile interaction and demonstrated that the static settlement of pile groups can be correctly estimated by superimposing the response of pile pairs. He also introduced the interaction factor concept in order to quantify pile-soil-pile interaction. Afterwards, Dobry and Gazetas (1988) studied this method for assessing the dynamic behaviour of pile groups, proposing some expressions to determine the flexibilities of the source pile and the interaction factors. Then, they computed the dynamic group responses applying elastic superposition and they verified that the results obtained were in good agreement with those computed through more advanced models. Other works employ the interaction factors within Winkler models (Makris and Gazetas, 1992; Mylonakis and Gazetas, 1998a,b, 1999), in which the pile-soil interaction is modelled through springs in parallel with dashpots. Subsequent studies propose interaction factors to take into account the wave scattered diffraction (Luan et al., 2020; Zheng et al., 2023; Wu et al., 2024; Zhong and Meng, 2023), as well as equivalent linear interaction factors which account other non-linear effects (El Naggar and Novak, 1995). The aforementioned works study the dynamic behaviour of pile groups under vertical (Poulos, 1968; Zhong and Meng, 2023; Mylonakis and Gazetas, 1998a,b; Rotta Loria and Laloui, 2016) or horizontal loads (Dai et al., 2017; Makris and Gazetas, 1992; Wang et al., 2017; Wu et al., 2024; Luan et al., 2020; Mylonakis and Gazetas, 1999; El Naggar and Novak, 1995), or both ones (Kaynia, 1982; Dobry and Gazetas, 1988; Gazetas et al., 1993). Most of them are focused on comparing the vertical or horizontal, rocking, and cross-coupled dynamic impedances of pile groups that are computed through rigorous models with those determined with the elastic superposition procedure (Kaynia, 1982; Dobry and Gazetas, 1988; Gazetas et al., 1993; Mylonakis, 1995; El Naggar and Novak, 1995; Rotta Loria and Laloui, 2016). However, these works are carried out for the classical regular pile group arrangements of civil construction projects, and not for pile group configurations of jacket-supported OWTs, which are characterised for disposing hollow cylindrical steel piles arranged in a N-sides polygonal configuration. In addition, these studies focused on studying the horizontal or vertical behaviour of pile groups in a decoupled way, without analysing the coupling of the vertical component with the horizontal and rocking ones, as well as the contribution of this coupling and the lateral and vertical behaviour on the determination of each impedance function term.

To fill this gap, this work aims to enhance the understanding of the superposition method's applicability for estimating the different impedance functions of OWT pile group foundations. To achieve this, the contribution of each flexibility term related to both vertical and lateral behaviour is thoroughly analysed. Thus, the main objectives of this work are: firstly, to study the elastic superposition method in the determination of the impedance functions related to the lateral behaviour of pile groups for jacket-supported OWTs; secondly, to analyse how the different components of the pile-soil-pile interaction (horizontal, rotational, vertical, and coupled terms) affect each impedance function of the whole group. For these purposes, the present work proposes an algebraic approach for the elastic superposition method that takes into account all horizontal, vertical, and rocking interaction factors. By employing the proposed formulation, the contribution of each of these terms on the group impedance functions is studied. A previously developed continuum model (Álamo et al., 2016) is used to compute the necessary components: individual pile flexibilities and pile-soil-pile interaction factors. This model is also used to obtain the reference group impedance results for benchmarking the proposed approach. Finally, it is important to emphasize that results for the group vertical impedance functions are not included in this work, as they have been analysed in a recent work of the authors (Rodríguez-Galván et al., 2025). Exploring the applicability of the superposition method for estimating impedance functions of OWT pile foundations offers several advantages for soil-structure interaction modelling of these systems. First, the method is computationally efficient, as it reduces the complex pile group problem to the analysis of isolated piles and pile-pile interaction pairs, while still capturing the essential physics of soil-pile interaction. Consequently, the superposition method facilitates efficient and reliable soil-pile-structure

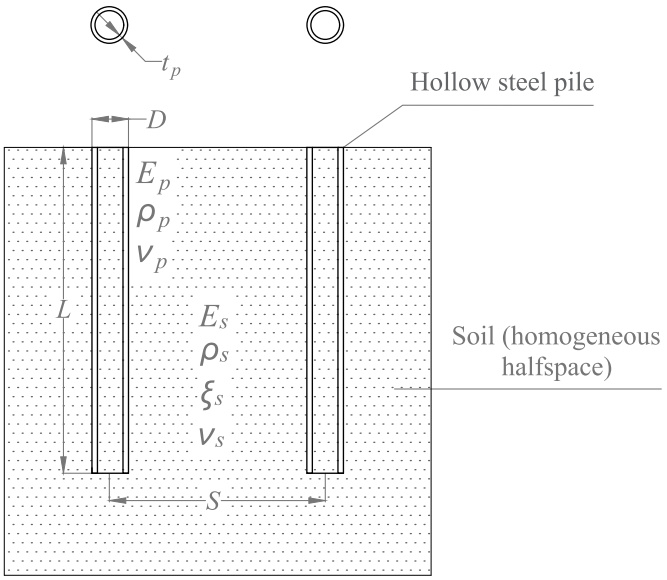

Fig. 1. Parameters involved in the dynamic problem under study (represented for a hollow pile pair).

interaction analyses for OWT design, avoiding the need for fully detailed and computationally intensive models to estimate the pile group dynamic behaviour. Note that preliminary designs and parametric studies are typically carried out using substructuring strategies, where a linear assumption of soil-foundation behaviour is considered an acceptable simplification.

The manuscript is structured in five sections. After this introduction, Section 2 shows the problem definition, exposing the parameters used to perform this study. Afterwards, Section 3 presents the matrix methodology based on the elastic superposition procedure to determine the pile group dynamic impedances. Then, Section 4 shows the main results and their discussion. Finally, Section 5 summarises the main conclusions of this work.

2. Problem definition

The dynamic problem under study is assumed to be frequency-dependent and will be addressed using a dimensionless approach. Thus, the eight following dimensionless parameters are used to define pile and soil characteristics: the dimensionless frequency (a_0):

$$a_o = \frac{\omega D}{V_s} \tag{1}$$

being D the pile diameter, ω the angular frequency, and V_s the shear wave velocity of the soil; the ratio between the separation among two piles and the pile diameter (pile spacing ratio, S/D); the relationship among the pile length and the diameter (pile slenderness ratio, L/D); the correlation of the Young's Modulus of the pile and soil (Young's Modulus ratio, E_p/E_s); the hysteretic soil damping (ξ_s); the relationship among the pile and soil density (density ratio, ρ_p/ρ_s); and, finally, the Poisson's ratios of piles and soil (ν_p and ν_s). All the physic variables are shown in Fig. 1 for a pile pair.

Piles are treated as hollow cylindrical foundations driven into a soil halfspace, which is assumed to be isotropic, elastic, and homogeneous. The assumption of homogeneous soil is initially introduced to evaluate the validity and applicability of the superposition method in estimating pile group impedance functions for OWT foundations. The pile and soil parameters, and the ranges used for them are listed in Table 1. The dimensionless frequency range is considered from 0.03 to 0.25. The upper value corresponds to a diameter equal to a quarter of the wave length, being within the range of application of the reference continuum model (Álamo et al., 2016). This value also ensures a sufficiently high frequency range to capture the earthquake frequency content. Different pile spacing ratios from 4 to 10 are analysed. These separations are representative of pile groups for jacket-supported OWTs, which are characterised by having large pile spacing relationships. The rest of dimensionless parameters are kept constant along the study, being their values also typical for jacket pile groups: a pile slenderness ratio of 20, representing a group composed of flexible piles; pile and soil Poisson's ratios of 0.25 and 0.40, typical values for structural steel and sandy soils respectively; a Young's Modulus ratio of 500; and a density ratio of 1.2. These last two values are the equivalent ratios obtained by considering a hollow steel cylindrical pile with soil mass in its inside. A pile thickness of 1.30 % of the diameter, based on the API (2014) recommendation and corresponding to an intermediate diameter value within the typical 1–3 m range for jacket OWT piles, is used to estimate these values. This choice has minimal influence on the dimensionless analysis, serving only to ensure that the Young's modulus and density ratios reflect typical pile-soil conditions for loose and soft sands. Finally, the hysteretic damping of the structural steel of the pile is not considered as its effects are negligible compared to the soil material and radiation damping.

Table 1
Dimensionless parameters considered in this study.

Parameter	Notation	Range/Value	Step
Dimensionless Frequency	a_o	[0.03 0.25]	0.001
Pile spacing ratio	S/D	[4 10]	2
Pile slenderness ratio	L/D	20	
Young's Modulus pile-soil ratio	E_p/E_s	500	
Density pile-soil ratio	ρ_p/ρ_s	1.2	
Soil hysteretic damping	ξ_s	1 %	
Pile Poisson's ratio	ν_p	0.25	
Soil Poisson's ratio	ν_s	0.40	

Four polygonal arrangements of pile groups composed of 2, 3, 4, and 5 piles are studied (see Fig. 2). Despite the fact that the group of 2 piles is not a real configuration for OWT structures, this arrangement is initially considered to study the influence of each flexibility term on the overall group flexibility. The other configurations are typical pile arrangements of pile groups for jacket supported OWTs. As shown in Fig. 2, a rigid connection is assumed between all piles of the group, a consideration close to reality taken into account that pile groups for jacket-supported OWTs are usually joined together with rigid beam framing (see, e.g., Zhang et al., 2025). Moreover, the annular space between the pile outer surface and the jacket leg inner surface is filled with high-strength grout, forming a joint that provides significant rotational stiffness and moment transfer (DNVGL-ST-0126, 2016).

3. Methodology

This section describes the matrix procedure followed to compute the impedance functions of the pile group, which is based on the elastic superposition method. As this study is performed in a dimensionless way, in Section 4, the flexibility and impedance functions are presented normalized by the pile diameter and Young's Modulus of soil. However, for simplification reasons, in this section the formulation is directly presented in the physical variables.

3.1. Matrix flexibility of the source and receiver pile

The elastic superposition method allows computation of the pile impedance functions through the sum of the responses obtained from two simple subproblems: a) a single isolated pile and b) a pair of piles (one loaded and one unloaded). Fig. 3 illustrates these two subproblems.

The first subproblem (Fig. 3a) corresponds to a single isolated pile i subjected to a dynamic load Q_s acting in the s direction. The response (displacement or rotation) of the pile in any r direction due to this load

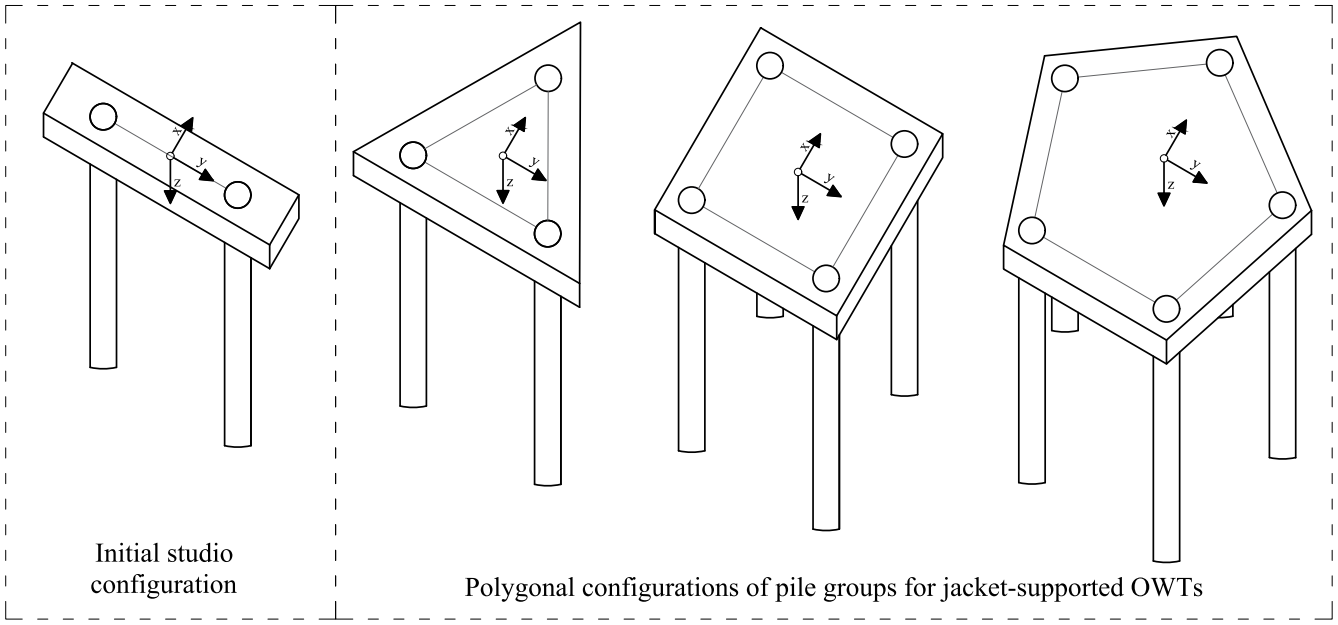

Fig. 2. Polygonal pile group configurations studied in this work.

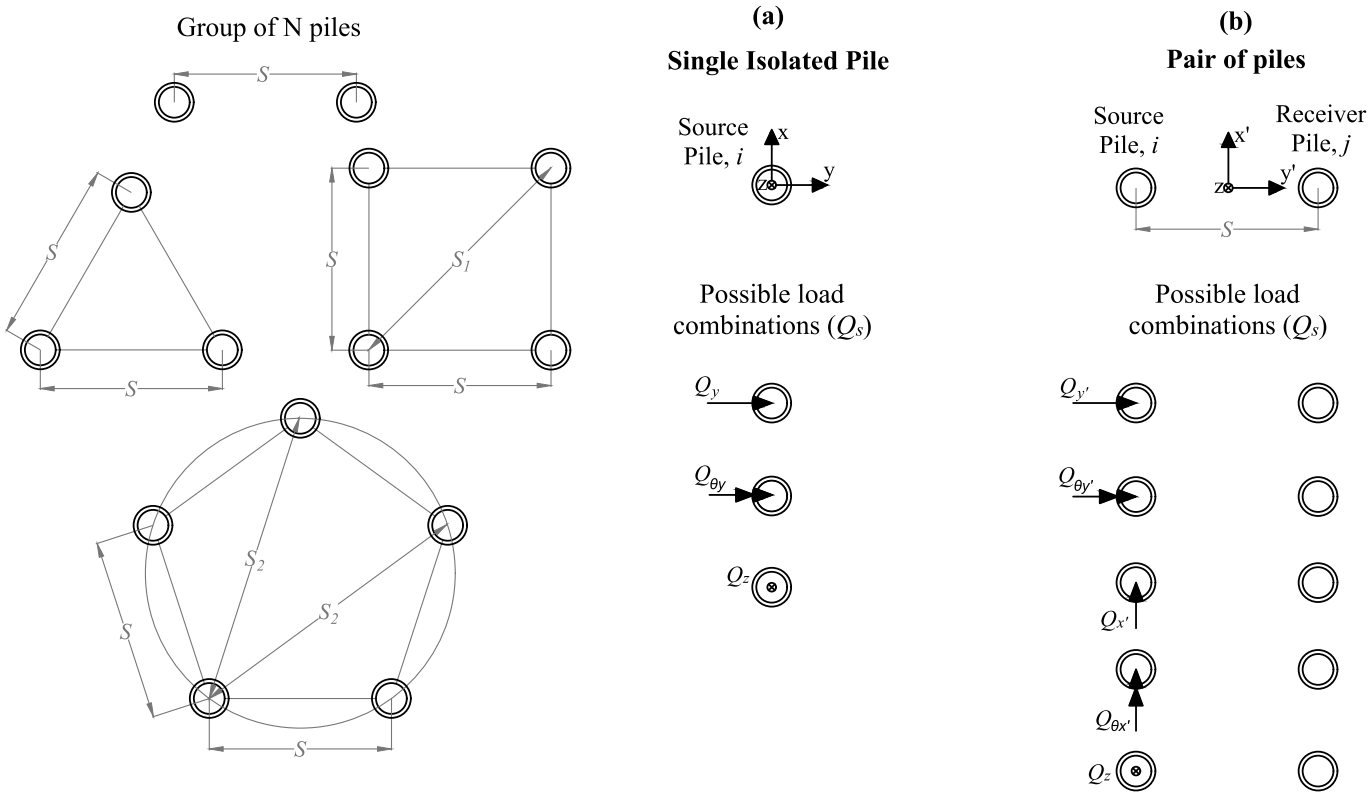

Fig. 3. Elastic superposition method subproblems with their possible load combinations (Q_s): (a) single isolated pile problem; (b) pair of piles problem.

is denoted as w_{rs}^{ii}. The flexibility of this single pile in the r direction as a consequence of the load acting over its head in the s direction is defined as:

$$F_{rs}^{ii}(\omega) = \frac{w_{rs}^{ii}(\omega)}{Q_s(\omega)} \tag{2}$$

Note that this flexibility term is a frequency-dependent complex value, whose real and imaginary parts represent the components of the response that are in-phase and out-of-phase with the acting load, respectively. As the present work aims to propose a general procedure which accounts all components, the directions of loads and responses can correspond to a horizontal (x, y), vertical (z), or rotational (θ_x, θ_y)

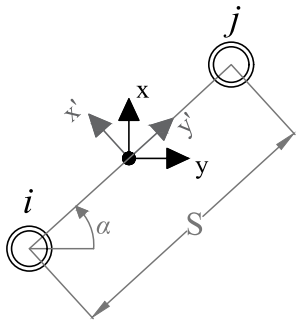

Fig. 4. Local ($x' - y'$) and global ($x - y$) coordinate systems for a pile pair.

problem. These flexibilities can be arranged in a 5x5 matrix that, due to the symmetry of the problem, can be completely defined with only the three load scenarios presented in Fig. 3a:

$$\mathbf{F_{ii}}(\omega) = \begin{bmatrix} F^{ii}_{yy}(\omega) & 0 & 0 & 0 & -F^{ii}_{y\theta_x}(\omega) \\ 0 & F^{ii}_{yy}(\omega) & 0 & F^{ii}_{y\theta_x}(\omega) & 0 \\ 0 & 0 & F^{ii}_{zz}(\omega) & 0 & 0 \\ 0 & F^{ii}_{y\theta_x}(\omega) & 0 & F^{ii}_{\theta_x\theta_x}(\omega) & 0 \\ -F^{ii}_{y\theta_x}(\omega) & 0 & 0 & 0 & F^{ii}_{\theta_x\theta_x}(\omega) \end{bmatrix} \tag{3}$$

The second subproblem (Fig. 3b) represents a pair of piles separated by a distance S, in which the pile i is the loaded, active or source pile, while pile j is the unloaded, receiver or passive one. The response of the source pile can be assumed to coincide with that of the isolated pile. The response of the receiver pile j in any r direction due to the load acting over the source pile head in the s direction is denoted w^{ji}_{rs}. Thus, the flexibility of the receiver pile j in the r direction caused by a load acting over the source pile i in the s direction is defined as:

$$F^{ji}_{rs}(\omega) = \frac{w^{ji}_{rs}(\omega)}{Q_s(\omega)} \tag{4}$$

For the pair of piles problem, each one of the five possible load situations presented in Fig. 3b have to be studied to completely define the flexibility matrix of the receiver pile:

$$\mathbf{F'_{ji}}(\omega) = \begin{bmatrix} F^{ji}_{x'x'}(\omega) & 0 & 0 & 0 & F^{ji}_{x'\theta_{y'}}(\omega) \\ 0 & F^{ji}_{y'y'}(\omega) & -F^{ji}_{zy'}(\omega) & F^{ji}_{y'\theta_{x'}}(\omega) & 0 \\ 0 & F^{ji}_{zy'}(\omega) & F^{ji}_{zz}(\omega) & F^{ji}_{z\theta_{x'}}(\omega) & 0 \\ 0 & F^{ji}_{y'\theta_{x'}}(\omega) & -F^{ji}_{z\theta_{x'}}(\omega) & F^{ji}_{\theta_{x'}\theta_{x'}}(\omega) & 0 \\ F^{ji}_{x'\theta_{y'}}(\omega) & 0 & 0 & 0 & F^{ji}_{\theta_{y'}\theta_{y'}}(\omega) \end{bmatrix} \tag{5}$$

Note that the vertical-lateral coupling components only correspond to those of the piles alignment direction y'. Then, the flexibility matrix of the receiver pile can be expressed in any global coordinate system ($\mathbf{F_{ji}}$) for a pile pair aligned in a direction rotated an angle α with respect to the global y-direction (see Fig. 4) through:

$$\mathbf{F_{ji}}(\omega) = \mathbf{L}^{\mathrm{T}}\mathbf{F'_{ji}}(\omega)\mathbf{L} \tag{6}$$

being $\mathbf{L}$ the coordinate transformation matrix:

$$\mathbf{L} = \begin{bmatrix} \cos\alpha & \sin\alpha & 0 & 0 & 0 \\ -\sin\alpha & \cos\alpha & 0 & 0 & 0 \\ 0 & 0 & 1 & 0 & 0 \\ 0 & 0 & 0 & \cos\alpha & \sin\alpha \\ 0 & 0 & 0 & -\sin\alpha & \cos\alpha \end{bmatrix} \tag{7}$$

3.2. Computation of the flexibility matrices

In this work, all flexibilities are determined through a previously developed linear-elastic continuum numerical model (Álamo et al., 2016). This model was designed to efficiently analyse pile foundations in layered soil under harmonic loading. It employs the integral reciprocity theorem and advanced Green Functions to simulate layered soils, accounting for free-field and inter-layer boundary conditions. Thus, radiation damping in the soil is directly incorporated into the formulation, without the need for artificial boundary conditions. Piles are modelled as load lines in the soil formulation, and their structural properties are incorporated by using beam finite elements (Padrón et al., 2007). This continuum elastic model can correctly simulate the dynamic behaviour of OWT's foundation elements, as validated in Álamo et al. (2021) through a comparison with a rigorous soil-shell model, demonstrating that the proposed soil-beam approach accurately captures the dynamic response of OWT foundations (piles and suction caissons) up to dimensionless frequencies of 0.5, i.e., when the foundation diameter equals half the wavelength. In any case, the proposed superposition methodology can be applied independently of the model used to compute the flexibility terms.

3.3. Group impedance calculation by superposition approach

Once the flexibility matrices of the source and all receiver piles of the group are obtained, the group impedance functions can be computed by superposition approach. Fig. 5 illustrates the superposition of the two subproblems for a horizontal load acting in the alignment direction of the piles ($s = y$) in a group of 2 piles. Note that, for the source pile (which is considered an isolated pile), the non-zero response directions corresponds to the horizontal displacement ($r = y$), and rotation around x-axis ($r = \theta_x$); while, for the receiver pile in the pair, the vertical displacement ($r = z$) is also considered.

The relationship between the displacements (and rotations) and forces (and moments) acting at the head of each one of the N piles within the group can be established through the overall flexibility matrix $\mathbf{F}$, which is composed of the flexibility matrices corresponding to each single pile and possible pile pair:

$$\begin{Bmatrix} \vec{w}_1(\omega) \\ \vec{w}_2(\omega) \\ \vdots \\ \vec{w}_N(\omega) \end{Bmatrix} = \begin{bmatrix} \mathbf{F_{11}}(\omega) & \mathbf{F_{12}}(\omega) & \cdots & \mathbf{F_{1N}}(\omega) \\ \mathbf{F_{21}}(\omega) & \mathbf{F_{22}}(\omega) & \cdots & \mathbf{F_{2N}}(\omega) \\ \vdots & \vdots & \ddots & \vdots \\ \mathbf{F_{N1}}(\omega) & \mathbf{F_{N2}}(\omega) & \cdots & \mathbf{F_{NN}}(\omega) \end{bmatrix} \begin{Bmatrix} \vec{Q}_1(\omega) \\ \vec{Q}_2(\omega) \\ \vdots \\ \vec{Q}_N(\omega) \end{Bmatrix} \tag{8}$$

where $\vec{w}_i$ and $\vec{Q}_i$ are the vectors containing the head displacement and forces of pile i:

$$\vec{w}_i(\omega) = \begin{Bmatrix} w^i_x(\omega) \\ w^i_y(\omega) \\ w^i_z(\omega) \\ w^i_{\theta_x}(\omega) \\ w^i_{\theta_y}(\omega) \end{Bmatrix}; \quad \vec{Q}_i(\omega) = \begin{Bmatrix} Q^i_x(\omega) \\ Q^i_y(\omega) \\ Q^i_z(\omega) \\ Q^i_{\theta_x}(\omega) \\ Q^i_{\theta_y}(\omega) \end{Bmatrix} \tag{9}$$

Eq. (8) can be expressed in a condensed form by grouping all pile head displacement and force vectors into the vectors $\vec{w}_p$ and $\vec{Q}_p$, respectively:

$$\vec{w}_p(\omega) = \mathbf{F}(\omega)\vec{Q}_p(\omega) \tag{10}$$

Note that these pile head displacements and forces are unknowns as, in general, the distribution of forces between piles can not be a priori established. In order to obtain their values, compatibility and equilibrium conditions at the pile cap are used.

In terms of compatibility conditions, as all piles are rigidly joined, the movements of each pile head can be related with the movement of

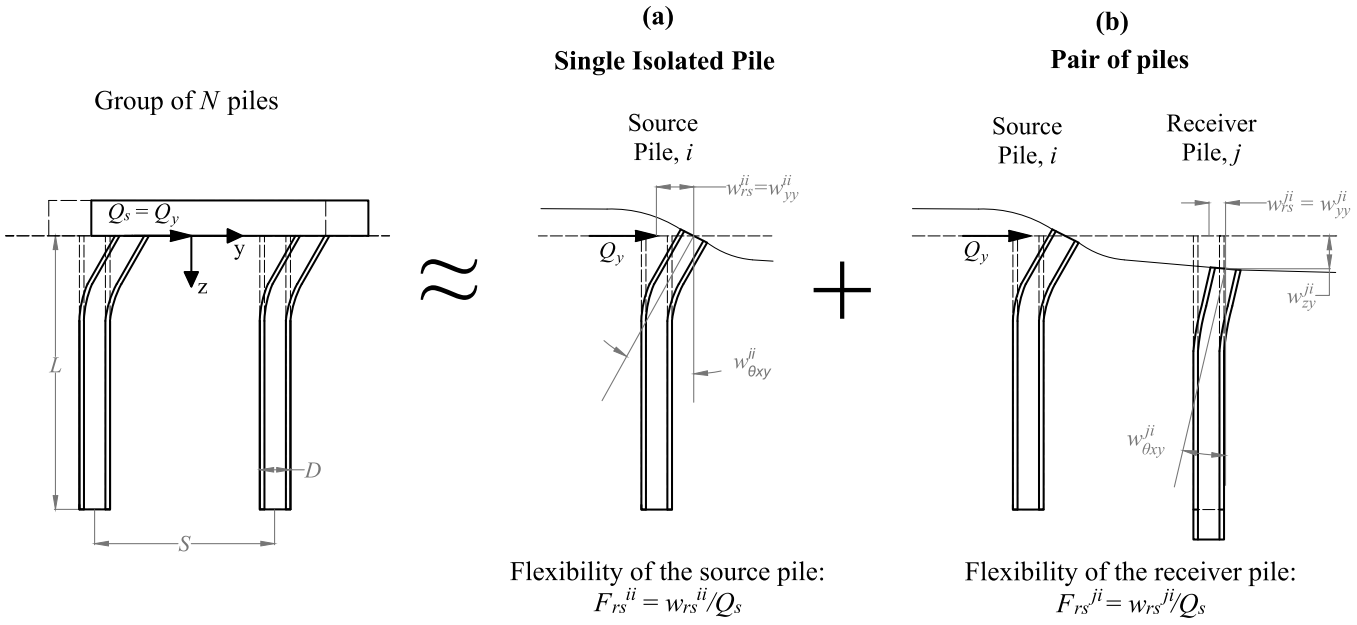

Fig. 5. Elastic superposition method for a horizontal load example ($Q_s = Q_y$). Displacements and flexibilities of the source (a) and receiver pile (b).

the gravity centre of the cap through:

$$\vec{w}_i(\omega) = \mathbf{H_i}\vec{w}_c(\omega) \tag{11}$$

being $\vec{w}_c$ the displacement vector of the gravity centre of the cap, and $\mathbf{H_i}$ the rigid linkage matrix between it and pile i:

$$\mathbf{H_i} = \begin{bmatrix} 1 & 0 & 0 & 0 & 0 \\ 0 & 1 & 0 & 0 & 0 \\ 0 & 0 & 1 & d_i^y & -d_i^x \\ 0 & 0 & 0 & 1 & 0 \\ 0 & 0 & 0 & 0 & 1 \end{bmatrix} \tag{12}$$

where d_i^y and d_i^x are the positions of pile i with respect to the gravity centre in each direction.

Assembling Eq. (11) for all piles within the group, the relationship between the pile heads displacement vector and the cap displacement vector is established through the total linkage matrix $\mathbf{H}$:

$$\vec{w}_p(\omega) = \mathbf{H}\vec{w}_c(\omega); \quad \text{with } \mathbf{H} = \begin{Bmatrix} \mathbf{H_1} \\ \mathbf{H_2} \\ \vdots \\ \mathbf{H_N} \end{Bmatrix} \tag{13}$$

On the other hand, neglecting the mass of the rigid cap, the external forces acting at the gravity centre of the cap $\vec{Q}_c$ should be in equilibrium with those at the head of each pile:

$$\vec{Q}_c(\omega) = \sum_{i=1}^{N} \mathbf{H_i}^{\mathrm{T}}\vec{Q}_i(\omega) = \mathbf{H}^{\mathrm{T}}\vec{Q}_p(\omega) \tag{14}$$

Finally, the system of equations that corresponds to the flexibility problem of the pile group is obtained by combining Eqs. (10), (13) and (14):

$$\begin{bmatrix} \mathbf{F}(\omega) & -\mathbf{H} \\ \mathbf{H}^{\mathrm{T}} & \mathbf{0} \end{bmatrix} \begin{Bmatrix} \vec{Q}_p(\omega) \\ \vec{w}_c(\omega) \end{Bmatrix} = \begin{Bmatrix} \vec{0} \\ \vec{Q}_c(\omega) \end{Bmatrix} \tag{15}$$

Solving this system, the relation between cap forces and displacements results in:

$$\vec{Q}_c(\omega) = \left(\mathbf{H}^{\mathrm{T}}\,\mathbf{F}^{-1}(\omega)\,\mathbf{H}\right)\vec{w}_c(\omega) \tag{16}$$

so, the group impedance matrix is directly obtained as:

$$\mathbf{K_G}(\omega) = \mathbf{H}^{\mathrm{T}}\,\mathbf{F}^{-1}(\omega)\,\mathbf{H} \tag{17}$$

and the group flexibility matrix can be computed as the inverse of the impedance matrix:

$$\mathbf{F_G}(\omega) = \mathbf{K_G}^{-1}(\omega) \tag{18}$$

Despite this matrix approach allowing the complete impedance and flexibility matrices of the pile group to be obtained, the system of Eq. (15) can be solved for a specific unitary load case to obtain either the distribution of forces between piles or the corresponding group flexibility terms.

As pile groups of jacket substructures present an axisymmetric behaviour, for the configurations composed of more than 2 piles (see Fig. 2), the impedance function matrix of the group can be expressed as:

$$\mathbf{K_G}(\omega) = \begin{bmatrix} K_H^G(\omega) & 0 & 0 & 0 & K_{HR}^G(\omega) \\ 0 & K_H^G(\omega) & 0 & -K_{HR}^G(\omega) & 0 \\ 0 & 0 & K_V^G(\omega) & 0 & 0 \\ 0 & -K_{HR}^G(\omega) & 0 & K_R^G(\omega) & 0 \\ K_{HR}^G(\omega) & 0 & 0 & 0 & K_R^G(\omega) \end{bmatrix} \tag{19}$$

being K_H^G, K_{HR}^G, K_R^G, and K_V^G the horizontal, cross-coupled, rocking and vertical dynamic stiffnesses of the group, respectively. Note the change of sign in the cross-coupled component due to the chosen reference system.

Finally, it is important to note that the pile cap mass has not been included in this study, since its effect can be introduced subsequently once the impedance function matrix has been obtained (Clough and Penzien, 1995).

4. Results and discussion

In order to address the objectives of this work, the results are organised as follows: firstly, all flexibility terms of both source (isolated) and receiver piles are presented. Afterwards, the different flexibilities of the 2-pile group computed by superposition and with the continuum model are analysed, evaluating the contribution of each flexibility term by analytically solving the problem. Finally, the horizontal, cross-coupled,

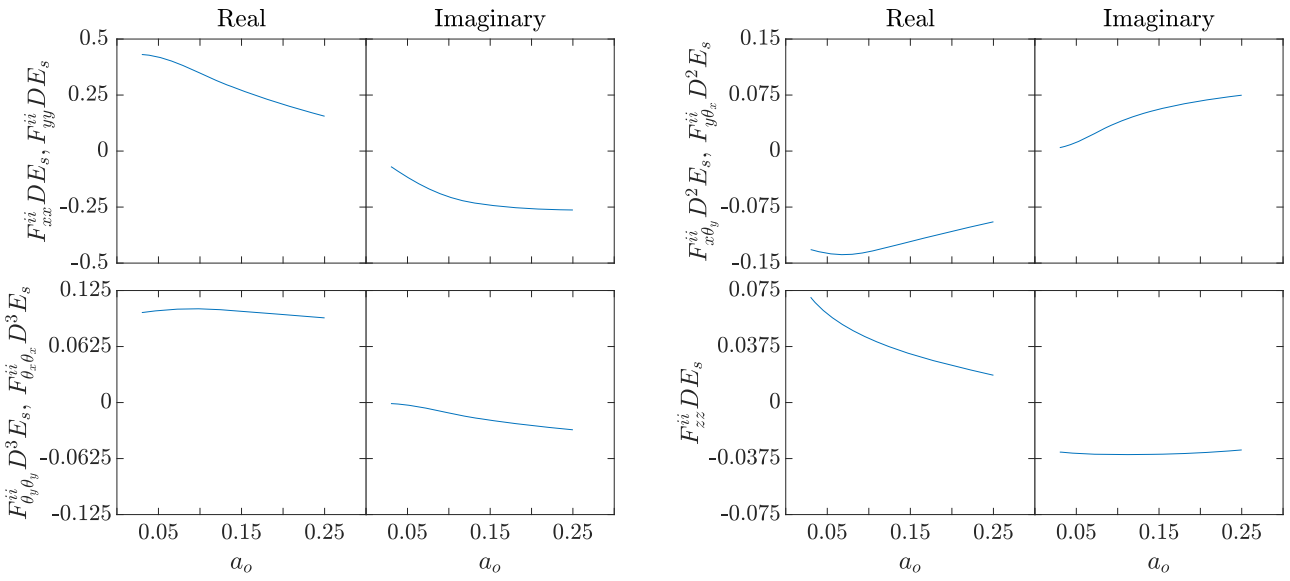

Fig. 6. Flexibility terms of the source pile.

and rocking impedances for jacket foundation's pile groups composed of 3, 4, and 5 piles computed by superposition are presented. Results are compared with those directly determined using the reference continuum model, and are used to study the influence of the flexibility terms corresponding to the lateral problem (horizontal, rocking, and their coupling), as well as the influence of the flexibility terms corresponding to the vertical problem (vertical and coupled terms with the lateral ones).

All results (flexibilities and impedances) shown throughout this section are presented in dimensionless form, normalized by the pile diameter (D) and Young's Modulus of the soil (E_s) (see, e.g., Kaynia and Kausel, 1991).

4.1. Flexibility terms of the source and receiver piles

Fig. 6 shows each term of the dimensionless flexibilities of the source pile (see Eq. (3)). The horizontal and cross-coupled flexibilities are depicted in the first row, while the rocking and vertical flexibilities are presented in the second one. Each flexibility term is arranged by pair of columns, showing the real and imaginary parts in the first and second column respectively. As it can be observed all flexibility terms of the source pile exhibit a slight curved variation with frequency. The real and imaginary parts of the horizontal, rocking, and vertical components have a decreasing behaviour with frequency, excepting the imaginary and real part of the vertical and rocking flexibilities accordingly, which mostly remain constant. On the other hand, the cross-coupled flexibilities present an increasing trend with frequency.

The different terms of the dimensionless flexibilities of the receiver pile (see Eq. (5)) are presented in Fig. 7. Each term of flexibility is shown by pair of graphs, in which its real and imaginary parts are depicted. The results computed for different pile spacing ratios (S/D = 4, 6, 8, and 10) are distinguished using several colours. As it is well known, all flexibility terms of the receiver pile present an oscillatory behaviour over the frequency range. This oscillatory trend is more pronounced in the lateral (x) and vertical (z) directions, both influenced by S-wave propagation, while the radial direction (y) is mainly affected by P-wave propagation. Furthermore, as it is expected, as pile spacing increases it is observed a reduction in the amplitude and an increment of the number of oscillations in the frequency range, resulting in a greater number of wavelength multiples within this range.

4.2. Contribution of each flexibility term over the global response of the 2-pile group

4.2.1. Lateral x-direction

By solving the system of Eq. (15) for the 2-pile group in the lateral x-direction (i.e. assuming either an unitary load in x-direction or moment around y-direction at the cap gravity centre), the horizontal, cross-coupled, and rocking group flexibilities are determined as:

$$F^G_{xx}(\omega) = \frac{F^{ii}_{xx}(\omega) + F^{ji}_{xx}(\omega)}{2} \tag{20}$$

$$F^G_{x\theta_y}(\omega) = \frac{F^{ii}_{x\theta_y}(\omega) + F^{ji}_{x\theta_y}(\omega)}{2} \tag{21}$$

$$F^G_{\theta_y\theta_y}(\omega) = \frac{F^{ii}_{\theta_y\theta_y}(\omega) + F^{ji}_{\theta_y\theta_y}(\omega)}{2} \tag{22}$$

Thus, in the x-direction and for the 2-pile group, the group flexibility terms only depend on their respective flexibility terms of the source and receiver pile. Note that the vertical component is decoupled from the x-direction behaviour for this 2-pile group. To illustrate this, Fig. 8 shows the dimensionless group flexibility terms related to the x-direction for the configuration of 2 piles. The horizontal, cross-coupled, and rocking group flexibilities are depicted by pair of columns at the first row, one column for the real part and another one for the imaginary term. The horizontal, cross-coupled, and rocking flexibilities of the source and receiver pile are presented in the second and third rows accordingly, presenting each of them by pair of columns in the same way as the group flexibilities. By employing different line styles, the group flexibilities computed directly through the continuum model (Direct, continuous lines) are distinguished from those obtained with the superposition methodology (SM, dashed lines). The results for two pile spacing ratios (S/D = 4 and S/D = 10) are shown by using different colours. It can be seen that the results obtained with the present superposition methodology align well with those directly computed by the continuum model for both pile spacing separations. Furthermore, it can be observed that the magnitude and trend of each group flexibility component are governed by the flexibility of the source pile, while the oscillation behaviour is introduced by the flexibility of the receiver pile. In other words, the oscillations of the flexibility group occur at the same frequencies at those of the receiver pile. These conclusions agree well with the previous expressions (Eqs. (20)–(22)), where each group flexibility term is obtained

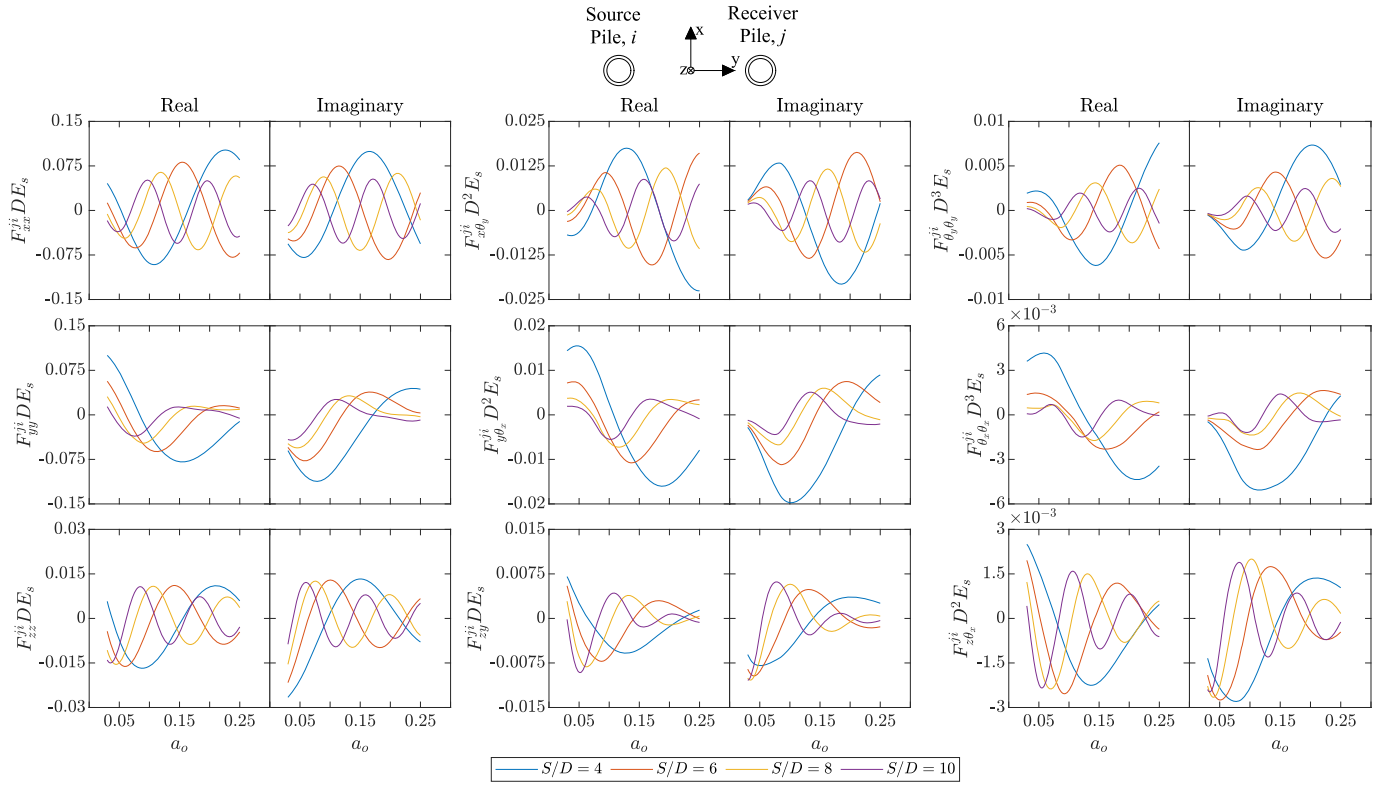

Fig. 7. Flexibility terms of the receiver pile for different pile spacing ratios.

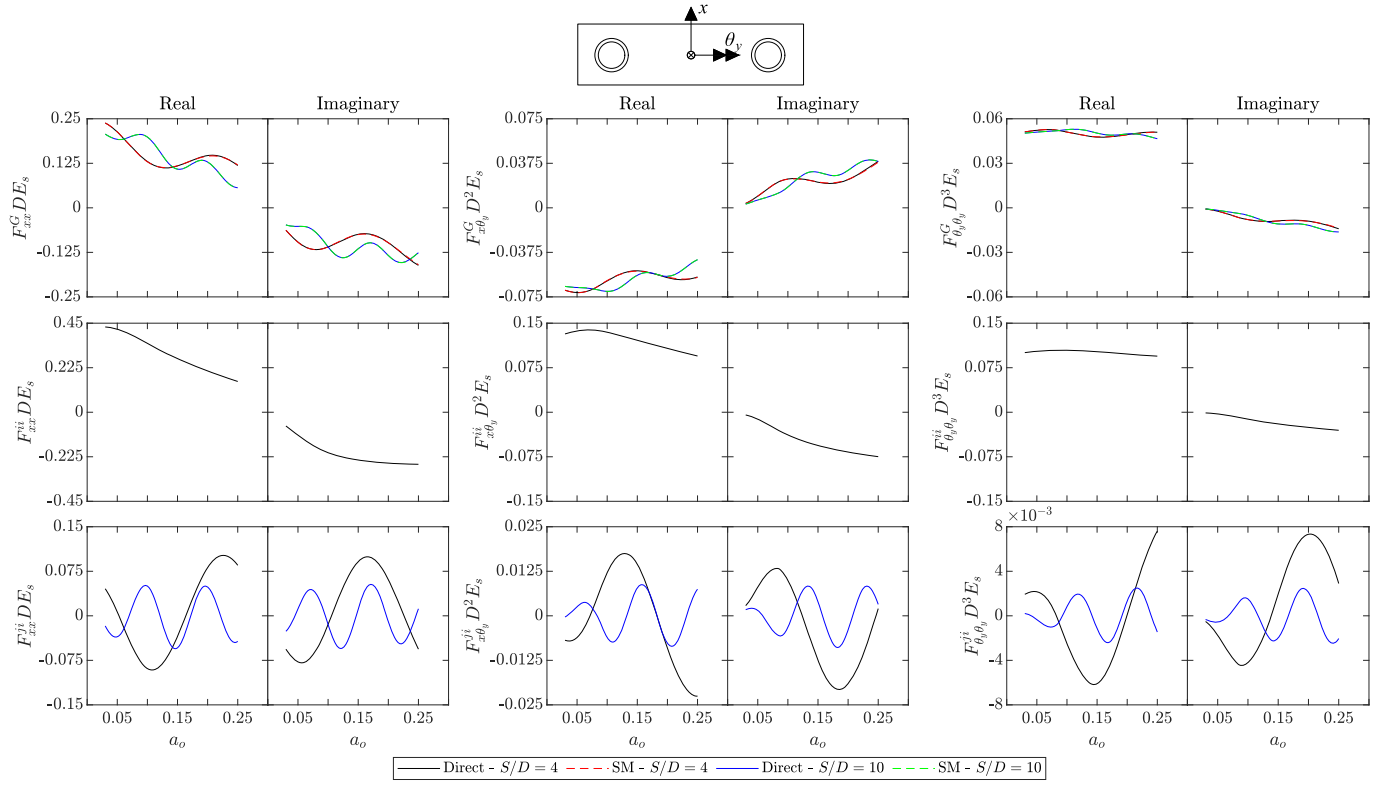

Fig. 8. Influence of the flexibility terms on the flexibility components of the 2-pile group (x-direction).

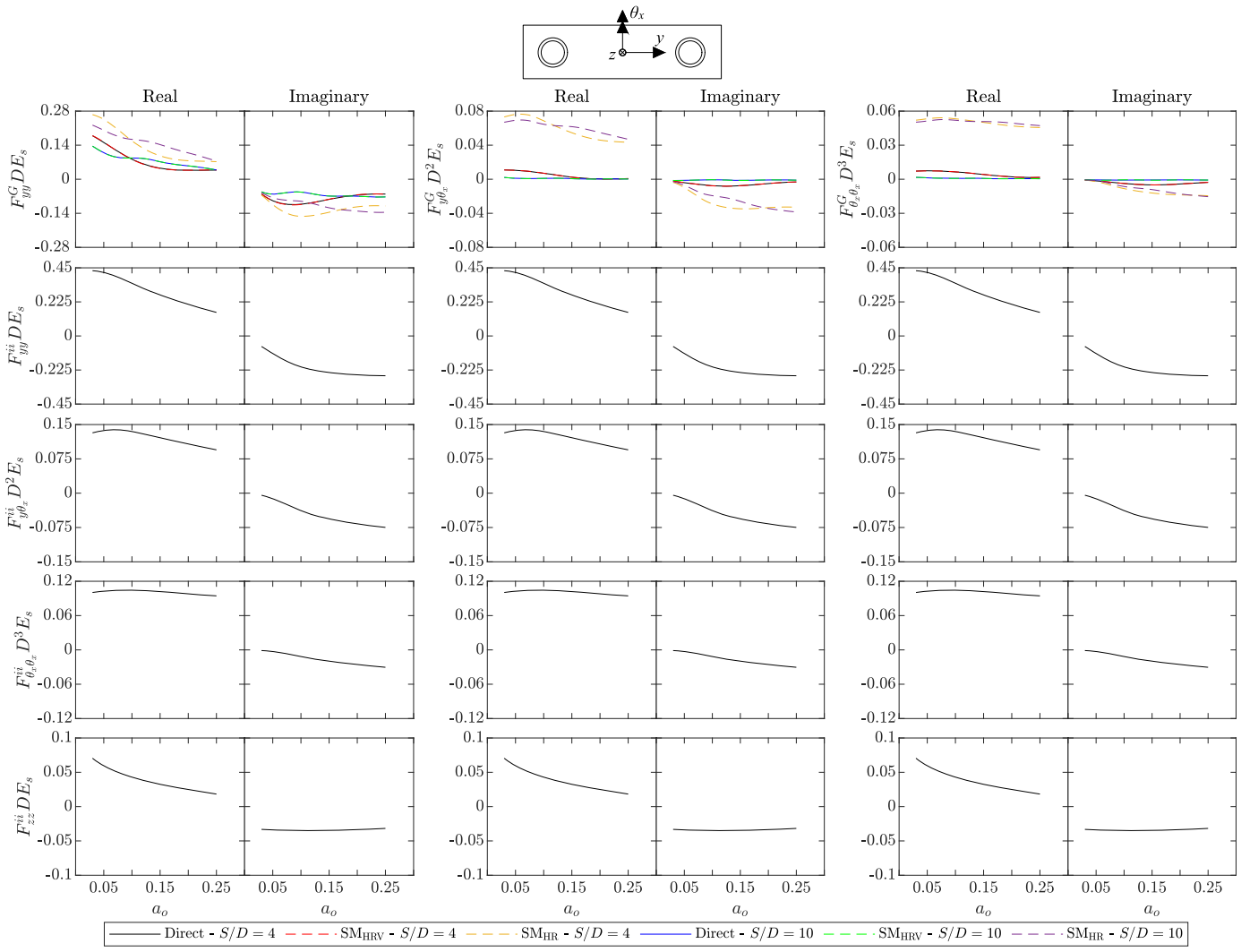

Fig. 9. Influence of the flexibility terms of the source pile on the flexibility components of the 2-pile group (y-direction).

through the sum of its respective source and receiver flexibilities. The study of this lateral x-direction behaviour for the 2-pile group is initially presented as a first step toward understanding its lateral y-direction behaviour, in which more components are involved.

4.2.2. Lateral y-direction

By addressing the system of Eq. (15) for the 2-pile group in the lateral y-direction (i.e. assuming either an unitary load in y-direction or moment around x-direction at the cap gravity centre), the expressions of the horizontal, cross-coupled, and rocking group flexibilities are obtained as:

$$F^G_{yy}(\omega) = \frac{-d^2 F_{y\theta_x}(\omega)^2 + d^2 F_{yy}(\omega) F_{\theta_x\theta_x}(\omega) + 2\, d F_{y\theta_x}(\omega) F_{zy}(\omega) - 2d F_{yy}(\omega) F_{z\theta_x}(\omega) - F_{zy}(\omega)^2 + F_{yy}(\omega) F_{zz}(\omega)}{2(d^2 F_{\theta_x\theta_x}(\omega) - 2d F_{z\theta_x}(\omega) + F_{zz}(\omega))} \tag{23}$$

$$F^G_{y\theta_x}(\omega) = \frac{-F_{zy}(\omega) F_{z\theta_x}(\omega) + F_{y\theta_x}(\omega) F_{zz}(\omega) - d F_{y\theta_x}(\omega) F_{z\theta_x}(\omega) + d F_{zy}(\omega) F_{\theta_x\theta_x}(\omega)}{2(d^2 F_{\theta_x\theta_x}(\omega) - 2d F_{z\theta_x}(\omega) + F_{zz}(\omega))} \tag{24}$$

$$F^{\theta_x\theta_x}_G(\omega) = \frac{F_{\theta_x\theta_x}(\omega) F_{zz}(\omega) - F_{z\theta_x}(\omega)^2}{2(d^2 F_{\theta_x\theta_x}(\omega) - 2d F_{z\theta_x}(\omega) + F_{zz}(\omega))} \tag{25}$$

being $d = S/2$ and each term F_{rs} refers to the sum of the corresponding flexibilities of the source and receiver piles:

$$F_{rs} = F^{ii}_{rs} + F^{ji}_{rs} \tag{26}$$

As expected, the y-direction behaviour of the 2-pile group is influenced by the vertical component. Therefore, in this direction, all terms are involved in the determination of the group flexibilities.

Figs. 9 and 10 depict the dimensionless group flexibility terms related to the y-direction for the configuration of 2 piles, and the different terms of the flexibility of the source pile (Fig. 9) and receiver one (Fig. 10). In the same way as in the previous Fig. 8, the horizontal, cross-coupled, and rocking group flexibilities are depicted in the first row by pair of columns (one for the real part and the other for the imaginary one). In the rest of rows, the different components of the source flexibility (Fig. 9) and the receiver one (Fig. 10) are presented. Results directly obtained through the model (Direct) are shown with a continuous line, while those computed through the proposed superposition methodology are presented with a dashed one. With the aim of analysing the influence of considering the terms related to the vertical component, two types of results obtained through the superposition methodology are presented: those taking into account all terms (horizontal, rocking, vertical, and their couplings: $\mathrm{SM_{HRV}}$ label); and those computed without considering the flexibility terms related to the vertical component (i.e., only contemplating the horizontal and rocking terms, and their

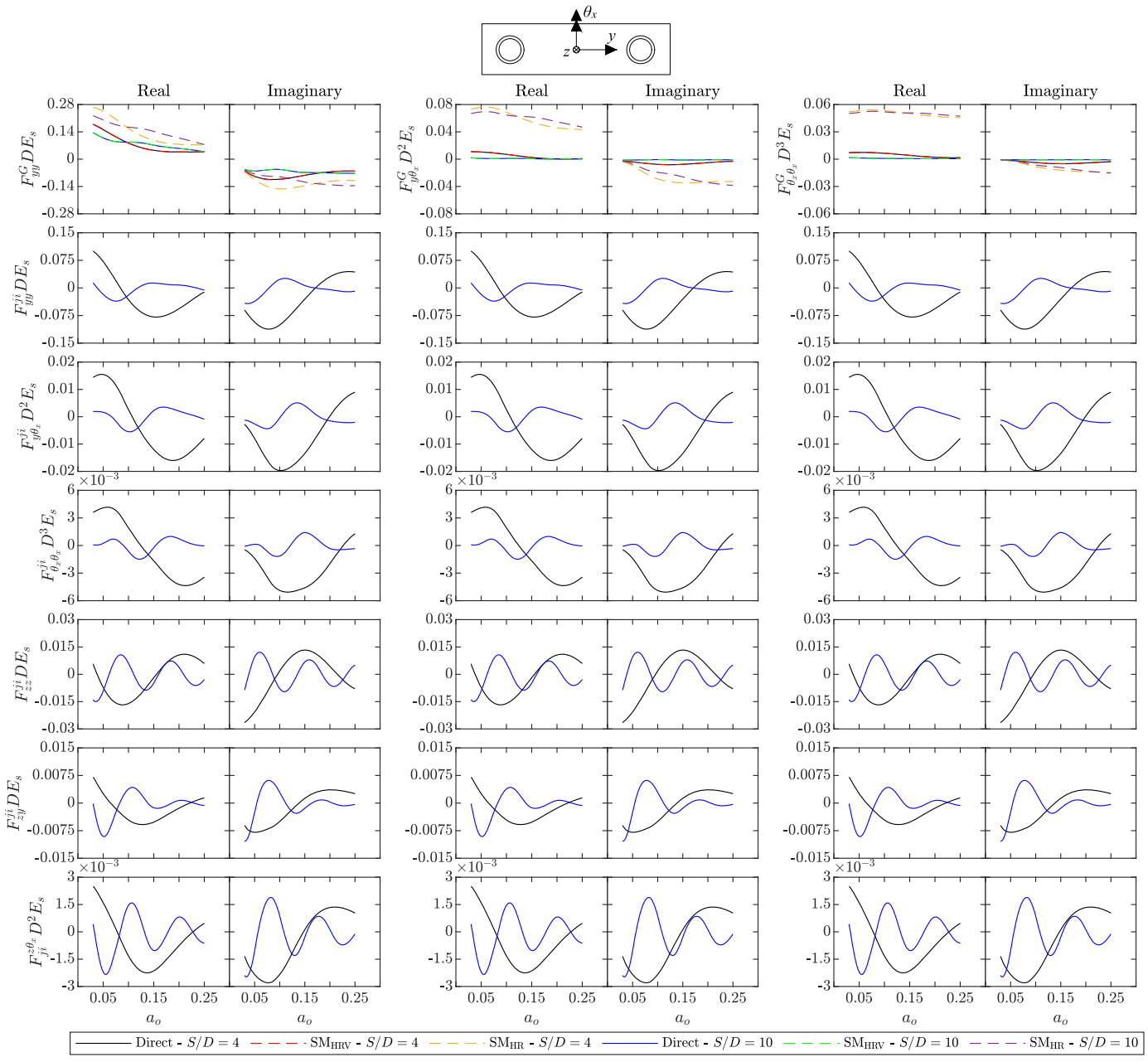

Fig. 10. Influence of the flexibility terms of the receiver pile on the flexibility components of the 2-pile group (y-direction).

couplings: SM$_{HR}$ label). Different colours are used to distinguish these two dashed lines, as well as the results corresponding to the pile spacing ratios of 4 and 10. At the first row of Figs. 9 and 10 it can be seen that it is necessary to consider the terms of the vertical component to correctly reproduce the group flexibilities, especially for the estimation of the cross-coupled and rocking ones. Note that the group flexibilities obtained with the superposition methodology align well with those of the direct model when the vertical component terms are contemplated. However, when these vertical terms are not considered, the different flexibilities of the group are not correctly replicated. In Figs. 9 and 10, it can be observed that the magnitude and trend of the group flexibilities are given by the flexibility of the source pile (Fig. 9). When the terms of the vertical component are not considered, it can be noticed a similar curve shape among each group flexibility curve and its respective flexibility of the source pile. However, when all vertical component terms are included, the curve shape of each group flexibility seems to be influenced by the shape of the vertical flexibility and its respective flexibility term of the source pile. From Fig. 10 it can be perceived that the frequencies in which the oscillations occur in the horizontal, cross-coupled, and rocking group flexibilities match approximately with those of their respective flexibility term of the receiver pile. This similarity of frequencies takes place in both situations: when the terms of the vertical component are considered and when they are not. Despite this, the group flexibilities computed for these two situations significantly differ between them. Thus, to correctly determine all group's flexibilities it is necessary to consider the flexibility terms related to the vertical component.

4.3. Horizontal, cross-coupled, and rocking dynamic group impedances

Fig. 11 shows the horizontal dimensionless impedance functions for the configurations of 3, 4, and 5 piles. Results corresponding to the pile spacing ratios of 4, 6, 8, and 10 are disposed by rows. The impedance functions of each pile group (3, 4, and 5 piles) are arranged by pair

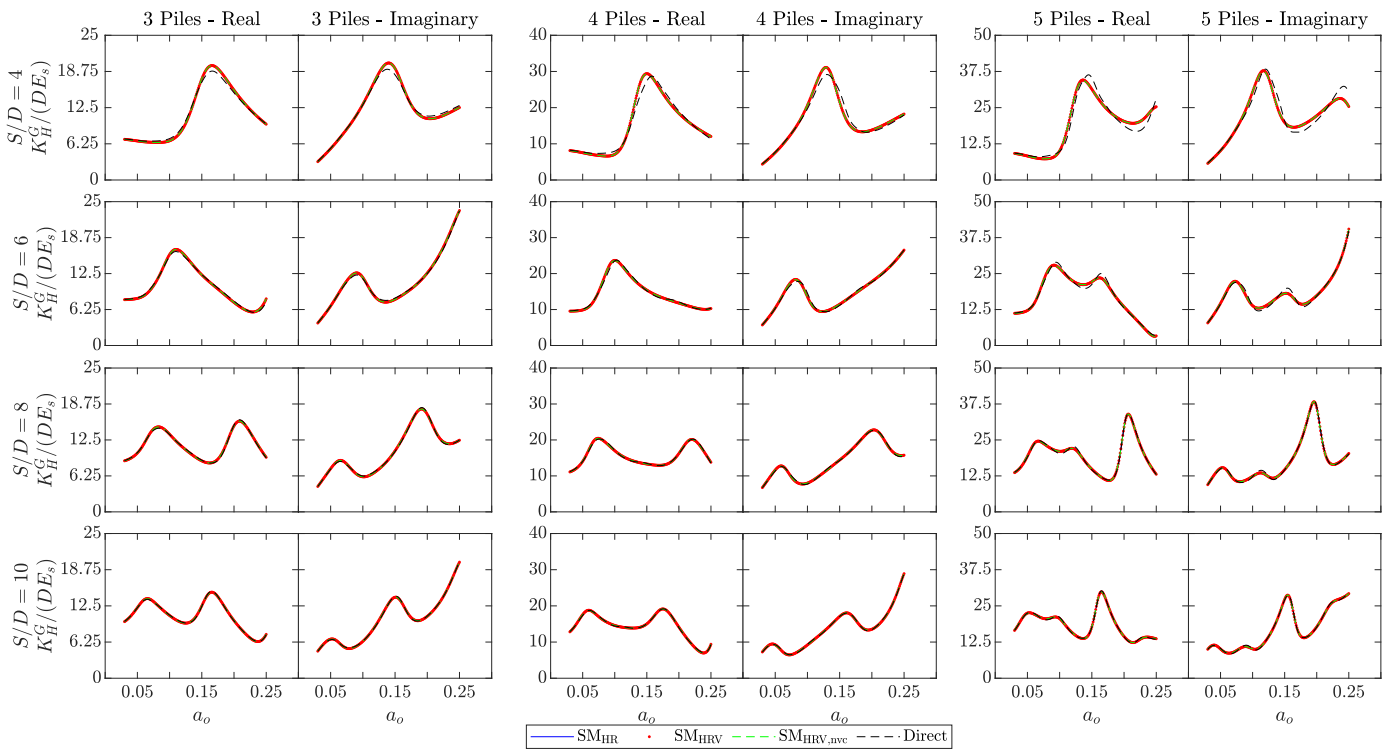

Fig. 11. Lateral dynamic group impedances for the configurations of 3, 4, and 5 piles.

of columns. The real and imaginary parts (stiffness and damping components) are depicted in the first and second column of each pair of columns, respectively. The impedance functions obtained through the superposition procedure by considering different flexibility components are distinguished by employing different colours and line styles: results obtained by only considering the horizontal and rocking flexibilities are presented with a blue trace (SM_{HR}); those considering all components of the matrix flexibility (horizontal, rocking, vertical, and their couplings) are presented with a red dotted curve (SM_{HRV}); and those computed by taking into account the horizontal, rocking, the coupling between these two, and the vertical flexibility (without considering the vertical-lateral couplings terms) are depicted with a green dashed line ($SM_{HRV,nvc}$). Results directly computed through the continuum model are represented with a dashed black line. From Fig. 11 it can be perceived that the horizontal impedances are correctly reproduced when all flexibility components are considered. Note how the red curve always matches well with the black one in all pile group configurations. For the lowest pile spacing ratio ($S/D = 4$), some discrepancies and phase differences are obtained between the direct model results and those of the proposed methodology (black and red curves) around the peaks of the curves. These differences are also greater for configurations with a larger number of piles. These discrepancies are due to the fact that the superposition method does not consider the interaction between all piles of the group, only the interplay among pair of piles. This interaction among all piles produces a scattering of waves that becomes more relevant as piles get closer to each other and as the number of piles in the group increases. Note that for pile spacing ratios larger than 4, these differences practically disappear, except in the 5-pile configuration, where small discrepancies can still be observed. Furthermore, the horizontal impedances are accurately estimated when the vertical coupling components are neglected (green dashed line) and when only the horizontal and rocking components are considered (blue line) in the superposition method (note how these lines align well with the direct model results, shown in black). Therefore, to correctly reproduce the horizontal impedance functions of this type of pile groups through the superposition method, it is enough to only consider the terms related to the horizontal and rocking components, without taking into account the vertical component.

Fig. 12 displays the cross-coupled dimensionless impedance functions for the configurations of 3, 4, and 5 piles. Results are depicted following the same layout as the previously used in Fig. 11. In Fig. 12 it can be observed that all terms (horizontal, vertical, rocking, and their couplings) must be included in the superposition procedure to accurately reproduce the cross-coupled impedance functions. Note that, for all configurations and pile spacing ratios, the red curve (which includes all terms) consistently matches the dashed black line (direct model results). It can be noticed that as the pile spacing ratio and the number of piles of the group increase, the coupling with the vertical component becomes more relevant. For the lowest pile spacing ratio ($S/D = 4$) and the 3- and 4-pile configurations (first and second column pairs in Fig. 12), the blue and green curves (which neglect coupling with the vertical component) approximately reproduce the cross-coupled impedances directly obtained from the continuum model. However, for larger pile spacing ratios, as well as for the lowest pile spacing ratio in the 5-pile configuration, these curves do not match with the direct model results, especially in lower frequencies and in the peaks of the cross-coupled impedance curve. In the same way as with the horizontal impedances (Fig. 11), comparing the results obtained using the superposition methodology (red curve) and those directly computed with the continuum model (black curve), some differences between them can be appreciated around their peak values for the small pile spacing ratios. As previously noted in the analysis of the horizontal group impedances, this arises from the simplification of the superposition procedure, which considers only pairwise pile interactions.

Fig. 13 shows the rocking dimensionless impedance functions for the configurations of 3, 4, and 5 piles. The results are presented using the same layout as in Figs. 11 and 12. Fig. 13 includes two more curves in each representation to better understand the lateral and vertical contributions on the rocking impedances: the rocking impedances obtained by only considering the vertical flexibility component are represented with an orange continuous line (SM_V label), which coincide with the

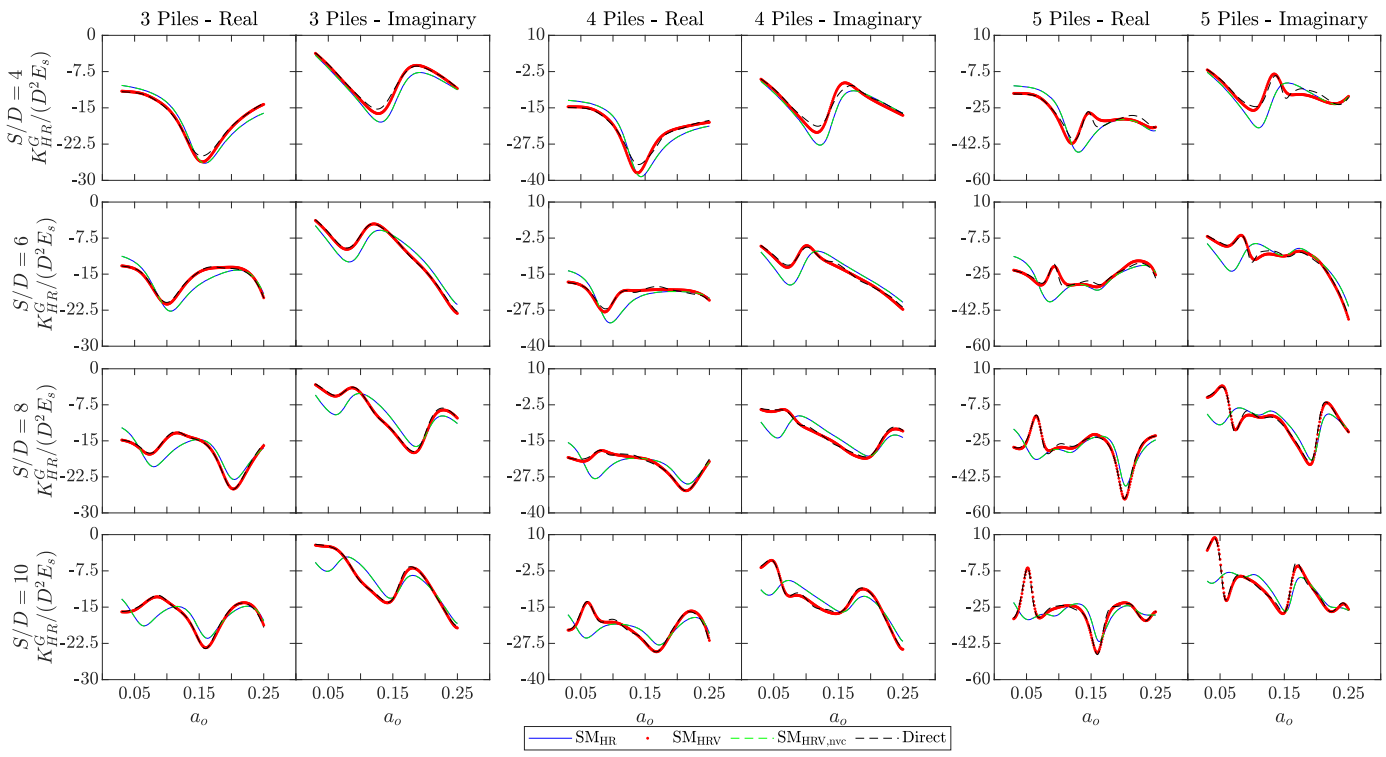

Fig. 12. Cross-coupled dynamic group impedances for the configurations of 3, 4, and 5 piles.

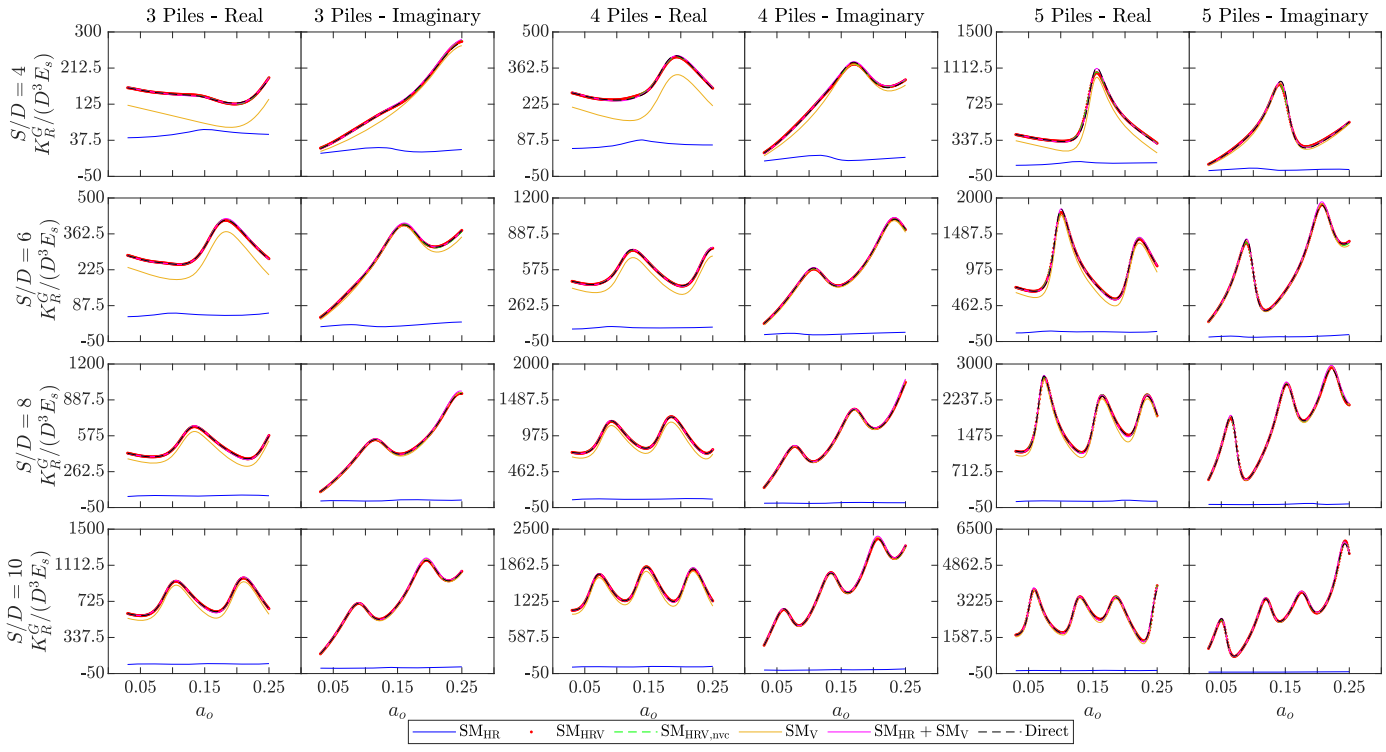

Fig. 13. Rocking dynamic group impedances for the configurations of 3, 4, and 5 piles.

methodology followed in Rodríguez-Galván et al. (2025); and those determined as the sum of the rocking impedances obtained by only considering the vertical contribution plus the ones computed by only contemplating the horizontal and rocking components are depicted with a magenta continuous line (SM$_{HR}$ + SM$_V$ label). In the same way as for the horizontal and cross-coupled impedances (Figs. 11 and 12), from Fig. 13 it can be noticed that the rocking impedances are accurately reproduced when all flexibility terms related to the horizontal, rocking, and vertical component are contemplated (red curve). Analysing the rocking impedances obtained by only considering the vertical flexibility term (orange continuous line), it is shown that this vertical component is clearly the dominant contributor to the rocking impedance function.

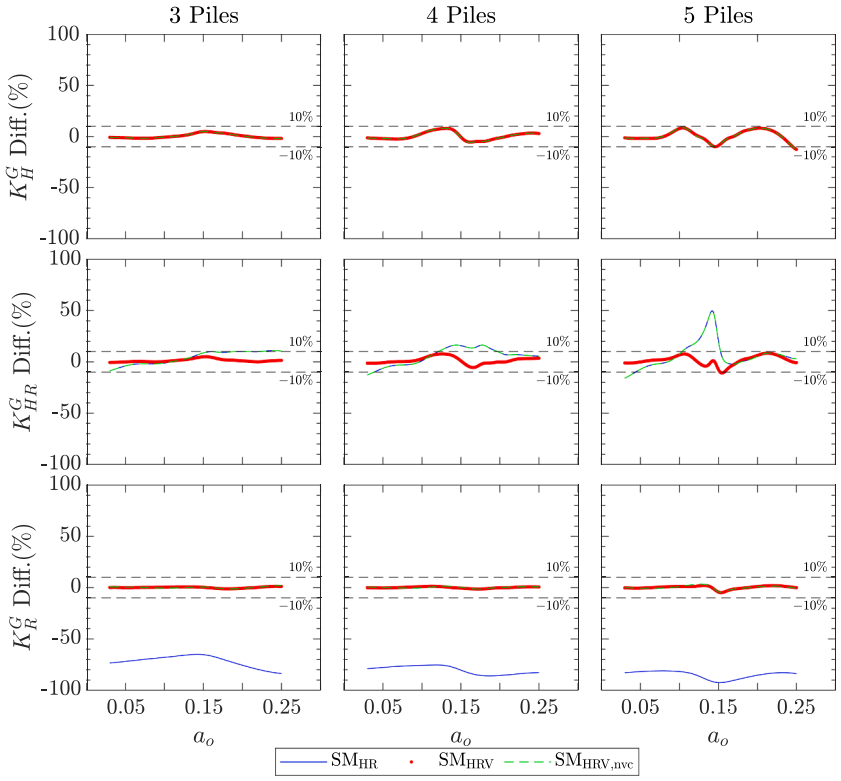

Fig. 14. Relative differences between the absolute values of the impedance functions computed using the superposition methodology and those directly obtained from the continuum model ($S/D = 4$).

Note how, as the pile spacing ratio and the number of piles increase, the orange curve increasingly aligns with the black curve (direct model results). By contrast, the contribution of the lateral behaviour to the rocking component is minimal, as evidenced by the blue curve, which consistently lies lower and shows significant deviation from the direct model results. The contribution of the lateral component is greater for the lower pile spacing ratios and the configurations with less number of piles (contrary to the vertical component influence). When the contribution of these two components (lateral and vertical) are separately added (green line), the rocking impedances are correctly reproduced, matching well with those directly computed with the continuous model and with the superposition methodology by contemplating all terms of the matrix flexibility (black and red lines accordingly). Moreover, the rocking impedances computed when all terms are considered excepting the couplings related to the vertical component (green curve, SM$_{HRV,nvc}$) closely match those obtained directly from the continuum model or from the superposition procedure considering all flexibilities. Therefore, to properly reproduce the rocking impedances via superposition, it is sufficient to consider all terms except the vertical-lateral coupling flexibilities.

Furthermore, it can be observed in all group impedance functions that their oscillatory behaviour increases as the number of piles and pile spacing ratio rises. This occurs as a consequence of the mutual interactions between piles. As the pile spacing ratio increases, the waves has more space to propagate and the interaction amplitude decreases, allowing piles to oscillate more freely. This fact can also be appreciated in Fig. 7. In addition, as the number of piles rises the interactions among piles also grows. Regarding the obtained trend in the different impedance functions with frequency, for the horizontal impedance (Fig. 11) it can be observed that the stiffness component has a general oscillatory decreasing behaviour with frequency, whereas the damping component has an increasing one. The decrease of the stiffness component with frequency is due to the reduced ability of the surrounding soil to deform in phase with the pile group as frequency rises, while the increase of the damping component arises from enhanced radiation of waves into the soil, leading to greater energy dissipation at higher frequencies. Concerning the rocking impedance (Fig. 13) it can be noted that this one has a highly oscillatory behaviour, which is because rocking movement excites more complex wave fields (a combination of S and P waves, as well as mode coupling) than horizontal motion. Attending to the cross-coupled impedance function (Fig. 12) this one presents an oscillatory behaviour, but with an intermediate nature: more complex than the horizontal impedance but less pronounced than the rotational one. This is due to this component simultaneously involves the dynamic mechanisms of translation and rotation. All these aspects agree with well-established conclusions in the dynamic behaviour of pile groups (such as Kaynia, 1982).

Finally, to quantify the differences obtained by using the presented methodology with respect to the continuum model, the relative differences between the absolute values of the impedance functions derived from the presented methodology and those directly computed from the continuum model are presented in Fig. 14. The relative differences are shown across the entire frequency range for the lowest pile separation ratio ($S/D = 4$), which corresponds to the case with the largest deviations. Differences computed for the three pile groups are arranged by columns, whereas the differences corresponding to the horizontal, cross-coupled and rocking impedances are shown in the first, second and third rows, respectively. Maintaining the same colour scheme and line styles used throughout the work, the relative differences obtained using the proposed methodology are illustrated as follows: those considering only horizontal and rocking flexibilities are shown with a continuous blue line (SM$_{HR}$); those including all components are represented by a red dotted line (SM$_{HRV}$); and those computed by excluding vertical-lateral coupling effects are depicted with a green dashed line (SM$_{HRV,nvc}$). As shown in Fig. 14, the maximum relative errors obtained with the proposed superposition approach when all flexibility components are considered (red line) are under an engineering-acceptable threshold of 10 % (horizontal dashed lines). These maximum values correspond to the pile groups with 4 and 5 piles. As observed in the previous figures,

these maximum differences occur at or near the frequencies where the peak values of the impedance functions are reached. Lastly, it is important to emphasize the relevance of considering the vertical-lateral coupling in the estimation of the cross-coupled impedance, as well as the significant contribution of the vertical component in the rocking impedance estimation. Note that significant relative differences arise when the vertical-lateral coupling term and the vertical component are neglected in the cross-coupled and rocking impedance functions, respectively.

5. Conclusions

This study explores the application of the superposition method for computing the impedance function matrix of OWT pile group foundations, focusing on the contribution of each flexibility term associated with the lateral and vertical behaviours in each impedance function. For this purpose, a matrix methodology based on the elastic superposition method is presented. Apart from considering the terms related to the horizontal and rocking components, the procedure also includes those related with the vertical component. The estimation of the horizontal, rocking, and cross-coupled impedances for this type of pile groups through the presented matrix procedure is analysed throughout the work. Furthermore, the contribution of the flexibility terms related to the lateral and vertical behaviour, as well as the coupling of the vertical and lateral problems is studied. Firstly, the flexibility terms and the influence of each of them on a 2-pile group flexibility has been analysed; afterwards, the horizontal, cross-coupled, and rocking impedance functions for pile groups composed of 3, 4, and 5 piles have been shown, comparing the results obtained with those directly computed using a continuum model. In order to study the influence of the terms related to the lateral and vertical behaviour, the impedance functions obtained with the presented superposition methodology have been computed by different ways: considering all terms (vertical, horizontal, and rocking ones, with all their couplings); contemplating all terms excepting the vertical-lateral couplings (vertical, horizontal and rocking terms, with the couplings of these last two); and considering only the components related to the lateral behaviour (horizontal and rocking terms, with their couplings). In addition, the influence of the isolated vertical term has also been studied for the rocking impedance functions. The main conclusions drawn of this work are:

- For the configuration composed of 2 piles, in both lateral directions (x and y), the magnitude and trend of each group flexibility term are mainly given by the respective flexibility of the source pile, while its oscillation behaviour is given by the respective flexibility of the receiver pile. The vertical flexibility of the source pile seems to affect the group flexibility curves related to the y-direction.
- The proposed matrix methodology based on elastic superposition accurately reproduces all impedance functions related to the horizontal and rocking behaviour of pile groups for jacket-supported OWTs. When all flexibility terms are considered in the matrix methodology, the horizontal , cross-coupled, and rocking impedance functions are accurately replicated.
- The horizontal impedance functions can be estimated without contemplating the vertical component. Thus, to compute the horizontal impedances it is enough to consider the terms related to the lateral behaviour (horizontal, rocking, and their respective couplings).
- To correctly estimate the cross-coupled impedance functions it is necessary to consider the vertical component, including its coupling with the horizontal and rocking terms. In this way, all terms (vertical, horizontal, and rocking, with all their couplings) must be contemplated for the cross-coupled impedance computations.
- The vertical flexibility component predominates in the computation of the rocking impedance function. However, for low pile spacing ratios ($S/D \leq 6$), it is necessary to also include the horizontal, rocking, and their respective coupling terms (without the vertical-lateral coupling) to accurately compute the rocking impedance.

Therefore, the horizontal, cross-coupled, and rocking impedance functions of pile groups for jacket-supported OWTs can be estimated with the proposed matrix methodology based on the elastic superposition method. Thus, the proposed methodology is well suited for the initial design phases or for conducting parametric analyses of this type of structure, where a large number of calculations and case studies need to be evaluated. Moreover, the simplifications summarised in the preceding points can be incorporated into the computation of each impedance function term, without compromising the accuracy of the resulting impedance functions. The correct estimation of these terms is an important factor to correctly reproduce the dynamic response of this type of structures. The understanding of the behaviour of these terms can serve as an estimation of the overall group dynamic behaviour, allowing the prediction of how the variation of different parameters affect the dynamic group impedances. The main advantage of this methodology is the direct computation of the pile group impedance functions from the behaviour of pile pairs, without the need to use a complex model. As future developments, it is suggested to use machine learning techniques (such as artificial neural networks) to obtain all flexibilities of the source and receiver piles from the main parameters that intervene into the problem (frequency, pile slenderness, Young's Modulus, pile-spacing ratios, soil hysteretic damping, pile and soil Poisson's ratios, etc). In this way, the flexibilities of the source and receiver piles could be obtained in a straightforward way, and the horizontal, cross-coupled, and rocking impedance functions could be later computed by employing the proposed methodology. In addition, future work could explore the application of the methodology to more realistic seabed conditions, including complex stratified soils or piles reaching a rigid bedrock, to assess how features such as soil layering, resonance effects, and tip constraints influence each pile-soil-pile flexibility term. It would also be valuable to evaluate the method's performance under non-linear behaviour (e.g., combining non-linear single-pile models with linear pile-to-pile interactions) to determine whether the superposition approach can estimate the overall system response within engineering-acceptable error margins.

CRediT authorship contribution statement

Eduardo Rodríguez-Galván: Writing – original draft, Visualization, Software, Methodology, Conceptualization; **Guillermo M. Álamo:** Writing – review & editing, Supervision, Software, Conceptualization; **Juan J. Aznárez:** Writing – review & editing, Supervision, Funding acquisition, Conceptualization; **Orlando Maeso:** Writing – review & editing, Supervision, Conceptualization.

Declaration of competing interest

The authors declare that they have no known competing financial interests or personal relationships that could have appeared to influence the work reported in this paper.

Acknowledgements

This research has been funded by the Ministerio de Ciencia Innovación y Universidades and the Agencia Estatal de Investigación (MICIU/AEI/10.13039/501100011033) of Spain and ERDF/EU through research project PID2023-151635OB-I00 and predoctoral research scholarship PRE2021-099200 (E. Rodríguez-Galván), also funded by FSE+. This research has also been partially supported by ACIISI, Spain-Gobierno de Canarias and ERDF Funds Grant EIS 2021 04.

References

Abhinav, K.A., Saha, N., 2015. Coupled hydrodynamic and geotechnical analysis of jacket offshore wind turbine. Soil Dyn. Earthq. Eng. 73, 66–79.

Álamo, G.M., Bordón, J.D.R., Aznárez, J.J., 2021. On the application of the beam model for linear dynamic analysis of pile and suction caisson foundations for offshore wind turbines. Comput. Geotech. 134, 104107.
Álamo, G.M., Martínez-Castro, A.E., Padrón, L.A., Aznárez, J.J., Gallego, R., Maeso, O., 2016. Efficient numerical model for the computation of impedance functions of inclined pile groups in layered soils. Eng. Struct. 126, 379–390.
Ali, A., De Risi, R., Sextos, A., 2021. Seismic assessment of wind turbines: how crucial is rotor-nacelle-assembly numerical modeling? Soil Dyn. Earthq. Eng. 141, 106483.
American Petroleum Institute, 2014. Recommended Practice for Planning, Designing, and Constructing Fixed Offshore Platforms–working Stress Design. American Petroleum Institute, Washington, D.C. 22 edition.
Bisoi, S., Haldar, S., 2015. Design of monopile supported offshore wind turbine in clay considering dynamic soil–structure-interaction. Soil Dyn. Earthq. Eng. 73, 103–117.
Clough, R.W., Penzien, J., 1995. Dynamics of Structures. Computers & Structures, Inc., Berkeley, CA, USA. third edition.
Dai, W., Shi, C., Tan, Y., Rojas, F., 2017. A numerical solution and evaluation of dynamic stiffness of pile groups and comparison to experimental results. Eng. Struct. 151, 253–260.
Dezi, F., Carbonari, S., Leoni, G., 2009. A model for the 3D kinematic interaction analysis of pile groups in layered soils. Earthq. Eng. Struct. Dyn. 38 (11), 1281–1305.
Dezi, F., Carbonari, S., Morici, M., 2016. A numerical model for the dynamic analysis of inclined pile groups. Earthq. Eng. Struct. Dyn. 45 (1), 45–68.
DNVGL-ST-0126, 2016. Support structures for wind turbines. Standard, Det Norske Veritas and Germanischer Lloyd.
Dobry, R., Gazetas, G., 1988. Simple method for dynamic stiffness and damping of floating pile groups. Geotechnique 38 (4), 557–574.
El Naggar, M.H., Novak, M., 1995. Nonlinear lateral interaction in pile dynamics. Soil Dyn. Earthq. Eng. 14 (2), 141–157.
Gazetas, G., Fan, K., Kaynia, A.M., 1993. Dynamic response of pile groups with different configurations. Soil Dyn. Earthq. Eng. 12 (4), 239–257.
Gazetas, G., Makris, N., 1991. Dynamic pile-soil-pile interaction. Part I: analysis of axial vibration. Earthq. Eng. Struct. Dyn. 20 (2), 115–132.
Global Wind Energy Council, 2024. Global Offshore Wind Report 2024. GWEC: Brussels, Belgium.
Jalbi, S., Bhattacharya, S., 2018. Closed form solution for the first natural frequency of offshore wind turbine jackets supported on multiple foundations incorporating soil-structure interaction. Soil Dyn. Earthq. Eng. 113, 593–613.
Kaynia, A.M., 1982. Dynamic stiffness and seismic response of pile groups. Ph.D. thesis. Massachusetts Institute of technology.
Kaynia, A.M., Kausel, E., 1991. Dynamics of piles and pile groups in layered soil media. Soil Dyn. Earthq. Eng. 10 (8), 386–401.
Kaynia, A.M., Pedersen, D.M., Askheim, H., Romero-Sánchez, C., 2025. Implementation of seismic soil-structure interaction in OpenFAST and application to an offshore wind turbine on jacket structure. Mar. Struct. 103, 103832.
Kim, D.H., Lee, S.G., Lee, I.K., 2014. Seismic fragility analysis of 5 MW offshore wind turbine. Renew. Energy 65, 250–256.
Luan, L., Zheng, C., Kouretzis, G., Ding, X., 2020. Dynamic analysis of pile groups subjected to horizontal loads considering coupled pile-to-pile interaction. Comput. Geotech. 117, 103276.
Makris, N., Gazetas, G., 1992. Dynamic pile-soil-pile interaction. Part II: lateral and seismic response. Earthq. Eng. Struct. Dyn. 21 (2), 145–162.
McCoy, A., Walter, M., Hammond, R., Hernando, D.M., Duffy, P., Beiter, P., Pérez, P., Baranowski, R., Reber, G., Spitsen, P., 2024. Offshore Wind Market Report: 2024 Edition. National Renewable Energy Laboratory (NREL), Golden, CO. Technical Report NREL/TP-5000-90525.
Medina, C., Álamo, G.M., Quevedo-Reina, R., 2021. Evolution of the seismic response of monopile-supported offshore wind turbines of increasing size from 5 to 15 MW including dynamic soil-structure interaction. J. Mar. Sci. Eng. 9 (11), 1285.
Mylonakis, G., 1995. Contributions to Static and Seismic Analysis of Piles and Pile-Supported Bridge Piers. State University of New York at Buffalo.
Mylonakis, G., Gazetas, G., 1998a. Settlement and additional internal forces of grouped piles in layered soil. Géotechnique 48 (1), 55–72.
Mylonakis, G., Gazetas, G., 1998b. Vertical vibration and additional distress of grouped piles in layered soil. Soil. Found. 38 (1), 1–14.
Mylonakis, G., Gazetas, G., 1999. Lateral vibration and internal forces of grouped piles in layered soil. J. Geotech. Geoenviron. Eng. 125 (1), 16–25.
Padrón, L.A., Aznárez, J.J., Maeso, O., 2007. BEM–FEM coupling model for the dynamic analysis of piles and pile groups. Eng. Anal. Bound. Elem. 31 (6), 473–484.
Padrón, L.A., Carbonari, S., Dezi, F., Morici, M., Bordón, J. D.R., Leoni, G., 2022. Seismic response of large offshore wind turbines on monopile foundations including dynamic soil–structure interaction. Ocean Eng. 257, 111653.
Plodpradit, P., Dinh, V.N., Kim, K.-D., 2019. Coupled analysis of offshore wind turbine jacket structures with pile-soil-structure interaction using FAST v8 and X-SEA. Appl. Sci. 9 (8), 1633.
Poulos, H.G., 1968. Analysis of the settlement of pile groups. Geotechnique 18 (4), 449–471.
Quevedo-Reina, R., Álamo, G.M., François, S., Lombaert, G., Aznárez, J.J., 2024. Importance of the soil–structure interaction in the optimisation of the jacket designs of offshore wind turbines. Ocean Eng. 303, 117802.
Rodríguez-Galván, E., Álamo, G.M., Aznárez, J.J., Maeso, O., 2025. An accurate and ready-to-use approach for the estimation of impedance functions of regular pile groups for offshore wind turbine foundations. Vertical and rocking components. Eng. Struct. 323, 119288.
Romero-Sánchez, C., Padrón, L.A., 2024. Influence of wind and seismic ground motion directionality on the dynamic response of four-legged jacket-supported offshore wind turbines. Eng. Struct. 300, 117191.
Rotta Loria, A.F., Laloui, L., 2016. The interaction factor method for energy pile groups. Comput. Geotech. 80, 121–137.
Shi, S., Zhai, E., Xu, C., Iqbal, K., Sun, Y., Wang, S., 2022. Influence of pile-soil interaction on dynamic properties and response of offshore wind turbine with monopile foundation in sand site. Appl. Ocean Res. 126, 103279.
Wang, J., Zhou, D., Ji, T.n., Wang, S., 2017. Horizontal dynamic stiffness and interaction factors of inclined piles. Int. J. Geomech. 17 (9), 04017075.
Wu, W., Di, T., Yang, X., El Naggar, M.H., Zhang, Y., 2024. Revised pile-pile mutual interaction factors for seismic analysis of end-bearing pile groups embedded in saturated stratum. Soil Dyn. Earthq. Eng. 182, 108745.
Yang, Y., Bashir, M., Li, C., Wang, J., 2019. Analysis of seismic behaviour of an offshore wind turbine with a flexible foundation. Ocean Eng. 178, 215–228.
Zhang, X., Wu, Y., Mantey, S.K., Gao, Y., He, B., Wang, Z., 2025. Optimized design of offshore wind turbine transition pieces through an information modelling approach and a hybrid optimization framework. Ocean Eng. 325, 120819.
Zheng, C., Cui, Y., Kouretzis, G., Luan, L., 2023. Scattered wave effects on the vertical dynamic response of pile groups embedded in layered soil. Comput. Geotech. 158, 105361.
Zhong, M., Meng, K., 2023. Dynamic interaction factor of pipe group piles considering the scattering effect of passive piles. J. Mar. Sci. Eng. 11 (9), 1698.